Many-body physics in small systems: Observing the onset and saturation of correlation in linear atomic chains

Emily Townsend [*]
Nanoscale Device Characterization Division, Joint Quantum Institute, National Institute of Standards and Technology, Gaithersburg, Maryland 20899-8423, USA and University of Maryland, College Park, Maryland 20742, USA

Tomáš Neuman [†]
Centro de Física de Materiales CFM-MPC, Centro Mixto CSIC-UPV/EHU, 20018 San Sebastián-Donostia, Basque Country, Spain; Donostia International Physics Center (DIPC), 20018 San Sebastián-Donostia, Basque Country, Spain; and Nanoscale Device Characterization Division, National Institute of Standards and Technology, Gaithersburg, Maryland 20899-8423, USA

Alex Debrecht
Nanoscale Device Characterization Division, Joint Quantum Institute, National Institute of Standards and Technology, Gaithersburg, Maryland 20899-8423, USA; University of Maryland, College Park, Maryland 20742, USA; and Department of Physics and Astronomy, University of Rochester, Rochester, New York 14627, USA

Javier Aizpurua
Centro de Física de Materiales CFM-MPC, Centro Mixto CSIC-UPV/EHU, 20018 San Sebastián-Donostia, Basque Country, Spain and Donostia International Physics Center (DIPC), 20018 San Sebastián-Donostia, Basque Country, Spain

Garnett W. Bryant
Nanoscale Device Characterization Division, Joint Quantum Institute, National Institute of Standards and Technology, Gaithersburg, Maryland 20899-8423, USA and University of Maryland, College Park, Maryland 20742, USA

(Received 13 November 2020; accepted 28 April 2021; published 20 May 2021)

The exact study of small systems can guide us toward relevant measures for extracting information about many-body physics as we move to larger and more complex systems capable of quantum information processing or quantum analog simulation. We use exact diagonalization to study many electrons in short one-dimensional atom chains represented by long-range extended Hubbard-like models. We introduce a measure, the single-particle excitation content (SPEC) of an eigenstate and show that the functional dependence of the SPEC on the eigenstate number reveals the nature of the ground state (ordered phases), and the onset and saturation of correlation between the electrons as Coulomb interaction strength increases. We use this SPEC behavior to identify five regimes as interaction is increased: A noninteracting single-particle regime, a regime of perturbative Coulomb interaction in which the SPEC is a nearly universal function of eigenstate number, the onset and saturation of correlation, a regime of fully correlated states in which hopping is a perturbation, and the SPEC is a different universal function of state number and the regime of no hopping. In particular, the behavior of the SPEC shows that when electron-electron correlation plays a minor role, all of the lowest-energy eigenstates are made up primarily of single-particle excitations of the ground state, and as the Coulomb interaction increases, the lowest-energy eigenstates increasingly contain many-particle excitations. In addition, the SPEC highlights a fundamental distinct difference between a noninteracting system and one with minute very weak interactions. Although the SPEC is a quantity that can be calculated for small exactly diagonalizable systems, it guides our intuition for larger systems, suggesting the nature of excitations and their distribution in the spectrum. Thus, this function, such as correlation functions or order parameters, provides us with a window of intuition about the behavior of a physical system.

DOI: 10.1103/PhysRevB.103.195429

[*]emily.townsend@nist.gov
[†]Present address: Institut de Physique et Chimie des Matériaux de Strasbourg, Université de Strasbourg, 23, rue du Loess, 67034 Strasbourg, France.

I. INTRODUCTION

Quantum simulation of small physically realizable systems (e.g., chains of precision-placed atoms on surfaces or dopant atoms in silicon) provides an opportunity to learn about many-body physics at larger scales. Although larger-scale quantum simulators with 50 to hundreds of atoms are becoming possible [1–3], the majority are still much smaller [4–8], particularly, in solid-state realizations. Studying these smaller systems theoretically has the advantage that we can exactly diagonalize their Hamiltonian, inspect the full spectrum of their eigenstates, and learn what both the ground and the excited states of that spectrum can reveal about the nature of the system. Even for small systems we gain insight into many-body behavior both from a theoretical perspective and with an eye toward experimental realization of quantum simulators for these systems. Hubbard model realizations are becoming a common stepping stone on the road to building universal quantum computers [9–12] and are being developed in ultracold atom systems in optical lattices [4] and solid-state systems, such as gate-defined quantum dots [5], and donor dots in semiconductors [6–8]. In this paper we use exact diagonalization of a small spinless electron system to find all of the many-body eigenstates, which gives us access to a wide range of exact quantities. We calculate the extent to which each of the eigenstates consists entirely of single-particle (s.p.) excitations of the ground state (GS) of the system, which we refer to as the single-particle excitation content (SPEC) of an eigenstate. Expanding our scope to all of the eigenstates provides a significant new perspective beyond what can be learned from examining only the ground state, in addition to confirming previously known ground-state behaviors in a new way. The SPEC of the excited states makes visible a fundamental difference between an unperturbed Hamiltonian and one with a minute perturbation, no matter how small. It also provides a division of the parameter space of our Hamiltonian into regimes which we can identify as those with different ground-state behaviors.

We work with a linear chain of atoms half-filled with spinless electrons, which we describe using a long-range-extended Hubbard model. By extended we mean that unlike a typical Hubbard Hamiltonian which has only on-site interactions between the electrons and a hopping kinetic energy, we use a Coulombic ($\sim 1/r$ with r as the distance between charges) interaction between electrons and between electrons and the atomic cores. We vary the ratio of Coulomb interaction strength λ_{ee} to the hopping t to examine the different regimes of behavior that this model gives rise to. As the Coulomb interaction is turned on it causes correlation between the electrons and then eventually strong Wigner crystallization that isolates electrons to individual sites of the lattice in an every-other-site pattern [13].

The range of the electron-electron interaction, whether short or long range, plays an important role in defining the physics of interacting systems. Long-range interactions allow the transfer of information and the spread of entanglement to exceed the Lieb-Robinson bound [14], which describes entanglement spread under only local interactions and implies our ability to efficiently simulate a one-dimensional (1D) system classically, e.g., using density-matrix renormalization-group (DMRG) or matrix product states [15]. In a 1D system with only nearest-neighbor hopping and interaction, information transfer will be local, the system integrable, and the system will not thermalize following a quench, whereas next-nearest-neighbor hopping and interactions break integrability, leading to quantum chaotic behavior and thermalization [16].

The strength of the interaction relative to the hopping is a key parameter which defines the phases of these systems. One-dimensional fermion systems have been studied extensively, e.g., Refs. [17–19], often with an emphasis on short-range interactions. When the fermions experience long-range Coulomb repulsion, Schulz [20] showed using bosonization that the ground state is a Wigner crystal (WC)-like state for a continuous infinite 1D region. The defining feature of this WC-like state is quasi-long-range order (quasi-LRO) in which the density-density correlation function shows an incipient charge-density wave (CDW) that decays slower than a power-law $\sim e^{-\sqrt{\alpha \ln x}}$ with $\alpha \sim t/\lambda_{ee}$, so with a stronger interaction the quasi-LRO decays more slowly. Although Schulz showed that this is the ground state at any strength of the Coulomb interaction, once a finite lattice of atomic sites is introduced there will be several different ground-state phases as one tunes the strength of interaction [21–24]. Different authors disagree on how to name these phases, but they broadly agree on many of their characteristics. Here we briefly describe the previous work but delay discussing these characteristics until the results section for ease of comparison.

In 1978, Hubbard [25] considered a Hubbard model with long-range but convex interactions and no hopping, which allows analytical solution by considering how to minimize the energy of placing m_e classical electrons on N_s sites. He named this ground state a generalized Wigner lattice. At half-filling the doubly degenerate ground states have electrons only on either odd or even sites. This corresponds to the $t = 0$ limit that we will discuss with our model.

When hopping is included, numerical solutions are typically needed. In 2000 Capponi *et al.* [21] considered spinless fermions with Coulomb repulsion on a lattice of varying lengths with periodic boundary conditions using exact diagonalization. By considering the thermodynamic limit of infinite chain length they investigated whether the system would be insulating or metallic and looked at how their numerical results departed from analytical predictions for a Luttinger liquid. More recently, Li [23] extended the work of Capponi by studying larger lattices also with periodic boundary conditions with long-range interactions of varying power laws, including a Coulombic $1/r$ using DMRG, rather than exact diagonalization. Finally, Ren *et al.* [24] used DMRG to study the phase diagram of the XXZ model of an anisotropic spin chain (a static 1D lattice of spin-1/2 particles with long-range interactions via Pauli spin matrices, also with periodic boundary conditions). Although their model should map to the interacting fermion model of Capponi [21] and Li [23], they do observe differences in the phase diagram, including a region of intermediate strength Coulomb interaction with the ground state in a phase that corresponds to Luttinger liquid behavior in the fermion system, a phase absent from Li [23] and Ren's [24] studies of fermions with long-range interactions.

In 2003, Valenzuela *et al.* [22] used a variational ansatz wave function to describe a smooth crossover between Hubbard's generalized Wigner lattice behavior and a state with weak charge-density modulation as well as delocalized charge. (For fillings smaller than 1/2 they also obtain a phase similar to to Schultz's [20] with quasi-LRO.) Their variational ansatz differs from the numerical approaches discussed so far, yielding only an approximation for the ground state but not any excited eigenstates.

This paper is organized as follows: Sec. I A on the model and methods describes the details of the Hamiltonian we study and defines both single-particle excitations and what we mean by the "single-particle excitation content" of an eigenstate. In Sec. II we then describe the behavior of the SPEC and show how the SPEC allows us to identify five regimes of behavior for different interaction strengths. These regimes are the noninteracting case, the no-hopping case, perturbative regimes around each of these cases, and the intermediate regime of onset and saturation of correlation. We finish with a conclusion in Sec. III.

A. Model and methods

We consider linear chains consisting of N_s atoms at fixed sites (indexed by i and j at positions x_i, x_j with unit spacing) with m_e spinless electrons moving from site to site via a nearest-neighbor hopping t. An electron on site i interacts Coulombically with the other electrons ($V_{\rm ee}$) and with the nuclei of each of the atoms ($V_{\rm nuc}$). Results presented here are for charge neutral systems in which each site has a nuclear charge of $Z = m_e/N_s$, so the attractive interaction between an electron at x_i and each of the atoms (at positions x_j) is

$$V_{\rm nuc}(x_i) = \sum_j \frac{-\lambda_{\rm nuc} Z}{(|x_i - x_j| + \zeta_{\rm nuc})}, \tag{1}$$

whereas the repulsive interaction between electrons at x_i and x_j consists of a direct Coulomb interaction reduced by exchange which we assume affects only nearest-neighbor electrons,

$$V_{\rm ee}(x_i, x_j) = \frac{\lambda_{\rm ee}(1 - f_{\rm ex}\delta_{|i-j|,1})}{(|x_i - x_j| + \zeta_{\rm ee})}, \tag{2}$$

where $\lambda_{\rm ee}$ and $\lambda_{\rm nuc}$ are scale factors accounting for the strength of these interactions, including any dielectric screening as well as the size of the lattice spacing. Variables $\zeta_{\rm ee}$ and $\zeta_{\rm nuc}$ are cutoffs that account for the spread of the electron orbital on a site. In all results presented here $\zeta_{\rm ee} = \zeta_{\rm nuc} = 0.5$ or half a lattice spacing. We assume each site has a single accessible orbital, so with spinless electrons each site can accommodate only one electron. The fraction by which the nearest-neighbor electron interaction is reduced due to exchange is $f_{\rm ex} = 0.2$ in the results presented here (but see the Supplemental Material [26] for results for other values of the exchange fraction as well as modifications of the range of the Coulomb/nuclear interaction, filling factor, and system size).

The full Hamiltonian is then,

$$\hat{\mathcal{H}} = \sum_{i=1}^{N_s} \left(-t(\hat{c}_i^\dagger \hat{c}_{i+1} + \hat{c}_{i+1}^\dagger \hat{c}_i) + V_{\rm nuc}\hat{n}_i + \sum_{j=1}^{i-1} V_{\rm ee}\hat{n}_i\hat{n}_j \right). \tag{3}$$

We express the Hamiltonian in a many-electron site basis and solve for the many-electron eigenstates and energies by direct diagonalization (LAPACK DSYEV). For comparison with theories of bulk materials, the value of the ratio $\lambda_{\rm ee}/t$ corresponds to the ratio of the Wigner-Seitz radius ($r_s = L/2m_e$) to the Bohr radius ($a_0 = \hbar^2/me^2$) (in which L is the length of the system, m_e is the number of electrons, $\hbar$ is Planck's constant, and m and e are the mass and charge of the electron). Thus, small $\lambda_{\rm ee}/t$ corresponds to the limit of high electron density and small Wigner-Seitz radius in which hopping is relatively more important than the Coulomb interactions.

1. Single-particle excitations

For zero Coulomb interaction, the many-electron eigenstates $\Psi_N(x_1, \ldots, x_{m_e})$ (where N is the many-electron eigenstate index and $x_1, \ldots, x_{m_e}$ are the position coordinates for the m_e electrons) are each a single determinant of m_e single-electron eigenstates (noninteracting modes) that are the solutions of the same system with one electron $\phi_n(x)$ (where n labels the single-particle eigenstates that make up the Nth many-electron eigenstate, and x is the position coordinate for a single electron),

$$\left\langle x_1, \ldots, x_n \middle| \Psi_N^{\lambda_{\rm ee}=0} \right\rangle = \frac{1}{\sqrt{m_e!}} \begin{vmatrix} \phi_{n_1}(x_1) & \cdots & \phi_{n_{m_e}}(x_1) \\ \vdots & & \vdots \\ \phi_{n_1}(x_{m_e}) & \cdots & \phi_{n_{m_e}}(x_{m_e}) \end{vmatrix}. \tag{4}$$

When the Coulomb interaction is turned on, the many-electron eigenstates are superpositions of many determinants with increasing departure from the single-determinant behavior as the interaction strength increases.

The single-particle excitation (SPE) of the many-electron ground state that takes a single particle from site j to site i can be written as

$$c_i^\dagger c_j |\Psi_{GS}\rangle, \quad i \neq j,$$

where $c_i^\dagger$ (c_i) is an operator that creates (destroys) a particle at site i. The set of all single-particle excitations is defined by the above states for all values of i and j. The full set can be equivalently defined by the states,

$$a_m^\dagger a_n |\Psi_{GS}\rangle, \quad m \neq n,$$

where $a_m^\dagger$ (a_m) instead creates (destroys) an electron in the noninteracting single-electron state ϕ_m. Similarly, a two-particle excitation of the ground state consists of $a_m^\dagger a_n^\dagger a_p a_q |\Psi_{GS}\rangle$, $m \neq n \neq p \neq q$ (or a similar construction with site creation and destruction operators).

A many-body excited state can be characterized by the number of one-, two-, three-, ... particle excitations that make it up. We show in this paper that the single-particle excitation content of the many-body excited states plays an important role, providing a way to characterize the effects of Coulomb interactions on the many-body states. We focus on the extent to which different many-electron eigenstates consist of single-particle excitations of the interacting ground state. For this purpose we define an orthonormal basis $|u_i\rangle$ that spans the full set of all single-particle excitations and a projection operator $\hat{P}_{SPE} = \sum_i |u_i\rangle\langle u_i|$, that projects onto that subspace. Computationally we find the spanning orthonormal basis by

Gram-Schmidt (G-S) decomposition: For each particular vector representing an excitation of the ground-state $c_i^\dagger c_j|\Psi_{GS}\rangle$, we create a basis vector $|u_{i'}\rangle$ by normalizing the vector that consists of the components of the excitation vector that are orthogonal to the ground state and to all previous basis vectors $|u_{i''}\rangle (i'' < i')$. (In the noninteracting case single-particle excitations will be eigenstates of the Hamiltonian and will already be orthogonal, but this is not true when interactions are present.) Because some of those components may be small, the normalization of the orthogonalized basis state has the effect of magnifying the components that are kept to make a new orthonormal basis state. We apply a cutoff, only including a new orthonormal basis state if the sum of the magnitudes of all of the components to be kept to make the new orthogonal basis state is, before normalization, greater than $\epsilon_{\text{G-S}}$. As we will discuss later, the choice of cutoff can affect our estimate of single-particle excitation content when interactions are weak and the interacting ground state includes many small single-electron excitations of the noninteracting ground state. Correct choice of cutoff is, thus, a regularization of the theory needed to get physically meaningful results: The cutoff needs to be chosen to exclude numerical error in the noninteracting and no-hopping cases, however, the most inclusive cutoff is the most accurate in other cases. If a more exclusive cutoff were used, the order that the single-particle excitations are included in the Gram-Schmidt process could affect (slightly) the SPEC, however, with an inclusive cutoff the answer is order independent. The size of the single-particle excitation basis $\{|u_i\rangle\}$ is $m_e(N_s - m_e)$ for a noninteracting system (or a system with no hopping) when the ground state consists of exactly m_e fully occupied modes (sites) and $N_s - m_e$ completely unoccupied ones and is $N_s^2 - 1$ for an interacting system with hopping when the ground state consists of modes or sites that are occupied with nonunity nonzero probability. There are N_s^2 combinations of $c_i^\dagger c_j$, but the ground state itself is not part of the single-particle excitation basis.

The SPEC of a particular many-electron eigenstate $|\Psi_N\rangle$ is then

$$\langle\Psi_N|\hat{P}_{SPE}|\Psi_N\rangle = \left|\sum_i \langle\Psi_N|u_i\rangle\right|^2. \tag{5}$$

The SPEC is, thus, the probability that an eigenstate can be found in the single-particle excitation subspace, or alternatively, the extent to which it can be defined entirely as a linear combination of single-particle excitations of the ground state. To simplify the display of the information contained in the plots of single-particle excitation content, we can also plot a rolling partial sum of the SPEC over the N-lowest many-body eigenstates,

$$\sum_{N'=1}^{N} \left|\sum_i \langle\Psi_{N'}|u_i\rangle\right|^2. \tag{6}$$

The single-particle excitation content is independent of which set of single-particle excitations we use, those from the site basis or the mode basis.

Because any linear combination of single-particle excitations will live entirely in this single-particle excitation subspace, the remaining subspace consists of correlated particle excitations in which two or more particles are moved coherently. The excitation $c_i^\dagger c_j c_k^\dagger c_l|\Psi_{GS}\rangle$ is distinct from the excitation $(c_i^\dagger c_j + c_k^\dagger c_l)|\Psi_{GS}\rangle$, the latter being entirely a single-particle excitation.

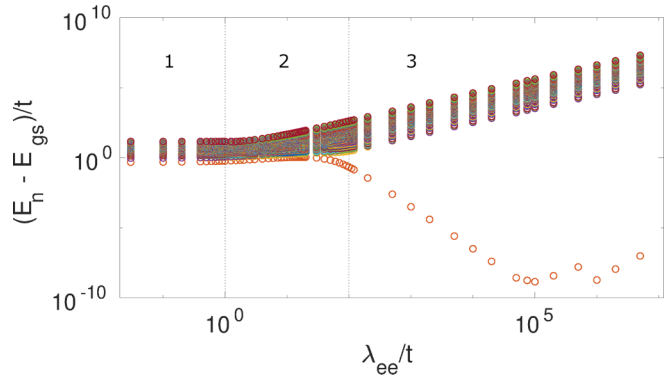

FIG. 1. Excitation energies (logarithm scale) for all many-body eigenstates of 6 electrons on a chain of 12 atoms, exchange fraction of 0.2. The horizontal axis is the ratio of the Coulomb interaction to the hopping on the logarithmic scale. Vertical dotted lines indicate regions of different behaviors discussed in the text.

The single-particle excitation content is distinct from but related to the quasiparticle weight. The relationship between the two is considered in the Supplemental Material [26] to this paper and references therein [27,28].

II. THE SPEC: IDENTIFYING FIVE REGIMES OF INTERACTION EFFECTS

In the following, we will show that the SPEC can be used to characterize the effects of the electron-electron interaction. We will show that there are five regimes of behavior identified by the very different functional form of the SPEC as a function of eigenstate number in each regime. As we vary the ratio of the electron-electron (and electron-nuclear) interactions to the hopping in the Hamiltonian for linear atomic chains, we use the behavior of the SPEC to identify two integrable cases ($\lambda_{ee}/t = 0$ and $t/\lambda_{ee} = 0$) and three regimes in between as suggested by the dashed lines in the plot (Fig. 1) of the variation of the excitation energy for excited states with λ_{ee}/t. (Figure 1 shows the difference in energy from the ground state on the logarithmic scale for all the excited states of six electrons on a chain of 12 atoms when the exchange reduction is 0.2. The horizontal axis is the ratio of the Coulomb interaction to hopping on the logarithm scale. Throughout the main paper we show plots for the half-filled 12 atom chain. However results are similar for other size chains, see the Supplemental Material [26].) In region 1, the excitation energies depend only weakly on the interaction strength. In region 2, the excitation energies exhibit significant increases with increasing interaction as well as significant crossings and mixings of levels. In region 3, the excitation energies scale linearly with the strength of the interaction as the hopping becomes much smaller than the interaction: Correlation saturates because movement of the electrons is suppressed. In addition, the ground state is becoming degenerate. We will discuss the noninteracting regime (Sec. II A), the no-hopping regime (Sec. II B), and then regimes 1 (Sec. II C), 3 (Sec. II D), and 2 (Sec. II E), in turn.

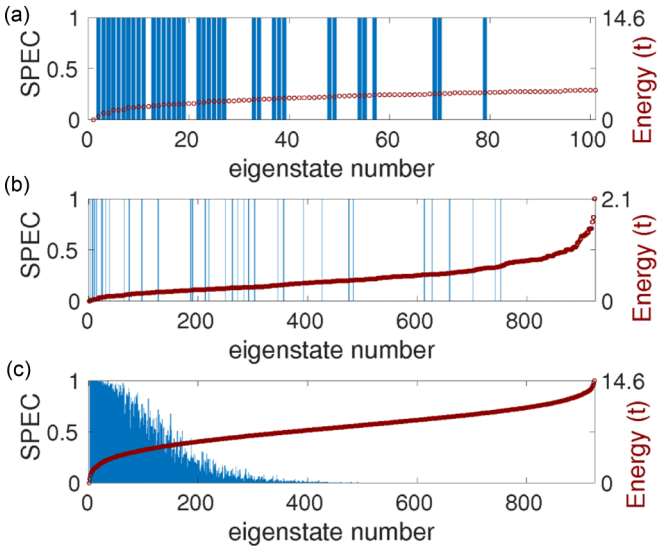

FIG. 2. Single-particle excitation content for eigenstates of a 12 atom chain with six electrons, $|\sum_i \langle \Psi_N | u_i \rangle|^2$ for (a) $\lambda_{ee} = 0$, $t = 1$ (no states above 100 have any single-particle content), (b) $t = 0$, $\lambda_{ee} = 0.5$, and (c) $\lambda_{ee} = t = 1$. There are $\binom{12}{6} = 924$ eigenstates for this system. The red line indicates the relative excitation energy of each eigenstate.

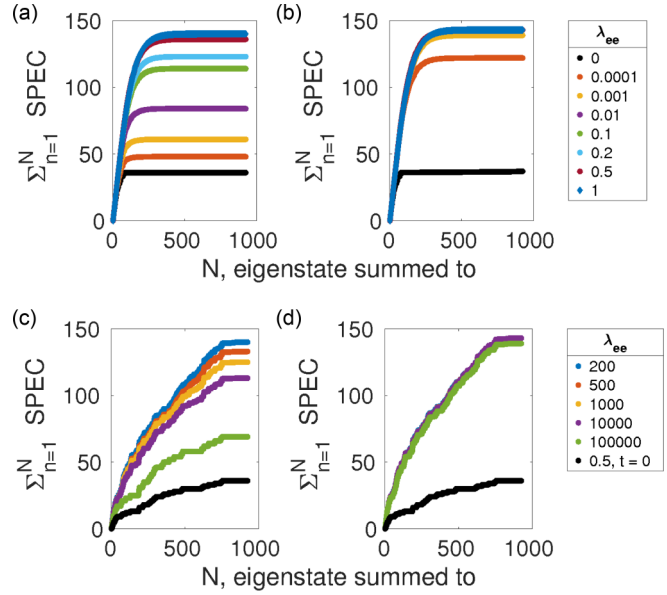

FIG. 3. Rolling sum of the single-particle excitation content for eigenstates of a 12 atom chain with six electrons for the perturbative regimes near the noninteracting state (upper two panels) and near the Wigner state (lower two panels). The right two panels have a more inclusive cutoff ($\epsilon_{G\text{-}S} = 10^{-18}$) whereas the left two panels have a more exclusive cutoff ($\epsilon_{G\text{-}S} = 10^{-7}$). With an inclusive cutoff, the SPEC curves are universal for a wide range of interaction strengths (curves overlap for many values).

A. Noninteracting regime $\lambda_{ee}/t = 0$

When there are no Coulomb interactions between electrons, the ground state consists of a single Slater determinant of the m_e lowest single-particle states of a finite 1D chain. Each excited state consists of a Slater determinant of single-particle states in which one or more of the m_e lowest single-particle states is replaced by a higher-energy single-particle state. Thus, each excited state consists entirely of either a single- or a multiple-particle excitation of the ground state. This is seen in Fig. 2(a) which shows the SPEC of the excited states of the noninteracting system of six electrons on a chain of 12 atoms. The eigenstates that are single-particle excitations (states 1–11, 13–19, etc.) have a SPEC of one, and all other states have zero SPECs. The partial sum of the SPEC of the N-lowest eigenstates, shown as the black curves in Figs. 3(a) and 3(b) rises to $m_e * (N_s - m_e)$ in the lower part of the spectrum of many-body eigenstates and then remains constant, indicating that all of the possible single-particle excitations are used up by the low-energy many-body states. This free-fermion regime can be described by a Luttinger liquid [29], whereas the inclusion of long-range interactions induces departures from Luttinger behavior [21]. Likewise, the SPEC for $\lambda_{ee}/t = 0$ with $m_e * (N_s - m_e)$ excitations is distinct from the SPEC for small λ_{ee}/t, even in the limit of very small λ_{ee}/t because there are always $N_s^2 - 1$ single-particle excitations when interactions are included.

B. No-hopping regime $t/\lambda_{ee} = 0$

When there is no hopping between sites, each eigenstate consists of a Slater determinant of single-particle states that are localized to sites. As discussed by Hubbard [25], the ground state is a Wigner crystal ("generalized Wigner lattice"), the exact details of which are determined by the exchange fraction f_{ex}, the number of sites, and the filling. For six electrons on 12 atoms with $f_{ex} = 0.3$ the ground state has electrons on sites 2, 3, 6, 7, 10, and 11, which we refer to as a paired Wigner crystal. When $f_{ex} = 0.2$ (or any value less than 0.22) the ground state is degenerate with one state having electrons on sites 2, 3, 5, 7, 9, and 11, and the other on sites 2, 4, 6, 8, 10, and 11. Sites 1 and 12 are not occupied in the ground state because the nuclear attraction pulls electrons toward the center of the chain. The states which are single-particle excitations (of just one of the degenerate ground states) are shown in Fig. 2(b). The partial sum of the the SPEC [the black curves in Figs. 3(c) and 3(d)] again shows that there are only $m_e * (N_s - m_e)$ single-particle excitations, although they are no longer confined to the lowest part of the spectrum since moving multiple electrons at the same time is often a lower-energy excitation. Again, the SPEC clearly shows that this regime is distinct from the large λ_{ee}/t limit where for interacting electrons there are $N_s^2 - 1$ single-particle excitations, no matter how strong the interaction.

C. Weak interaction $\lambda_{ee}/t \leqslant 1$

In the small interaction regime, the ground state is perturbed from the noninteracting ground state we discussed above. This can be seen in Fig. 4, which shows the ground-state expectation value of the single-particle excitation operator $a_m^\dagger a_n$ for the Coulomb interaction strength of zero and t. The diagonal elements show the occupancy of the noninteracting single-particle modes (one or nearly one for modes 1–6 and zero or nearly zero for modes 7–12). When the diagonal elements alone are plotted (see the Supplemental

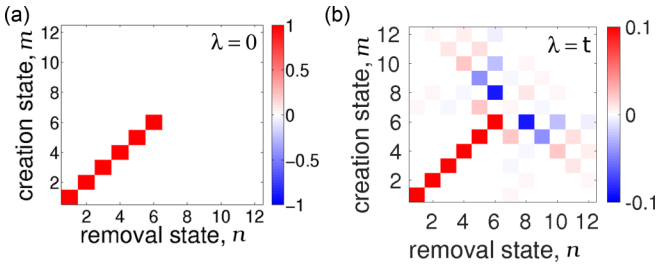

FIG. 4. The expectation value of the single-particle excitation operator in mode space (projection of the ground state onto the single-particle excitations of the ground state in the wave-function basis) $\langle \Psi_{GS} | a_m^\dagger a_n | \Psi_{GS} \rangle$ for (a) no interaction and (b) a Coulomb interaction equal to the hopping. Note the color scale differs between (a) and (b).

Material [26]) the mode occupancy is seen to be similar to a Fermi function with the noninteracting case a perfect step function, and the interactions smearing the Fermi sea similar to a finite temperature. The values of off-diagonal elements are zero for the noninteracting case and increase with the Coulomb strength as the ground state becomes dressed by the interaction.

The particular single-particle excitations of the ground state begin to mix together in linear combinations in this regime. This can be seen in Fig. 5 which shows the projection of the 12 lowest excited states onto each of the possible single-particle excitations (in the single-particle mode basis) of the ground state for $\lambda_{ee} = t$. The figure shows that the lowest-energy eigenstates consist of linear combinations of multiple single-particle excitations. In this regime the low-energy excitations are plasmonic [30]. The first excited state is made mostly from the one way to shift one electron from the highest occupied single-particle state to the first unoccupied single-particle state. The next two excitations are determined mostly by the two ways that one electron can be excited with a change in the single-particle index of two. These first three excitations correspond to the fundamental plasmon mode, the plasmon mode with two nodes, and the doubly excited fundamental plasmon mode [30]. Excitations with larger changes in single-particle index correspond to higher-order plasmon modes and other multiply excited plasmonic excitations.

In the weak interaction regime the SPEC is sensitive to $\epsilon_{G\text{-}S}$, the cutoff used to decide whether a particular single-particle excitation of the ground state has enough new orthogonal components to be included in the single-particle excitations basis. More basis states are included, capturing more of the SPEC if a smaller cutoff is used. Genuine but small perturbations in the ground state may be excluded or not depending on that cutoff, influencing the total number of single-particle excitations of the ground state that appear (saturation value of the curve). In this perturbative regime, the ground state consists of an unperturbed ground state mixed with the unperturbed excited states, making more single-particle excitations of the ground state possible. (This is because single-particle modes are no longer completely filled or completely empty.) However, the larger the interaction, the greater the mixing, and the less likely that any particular single-particle excitation of the ground state will be excluded by the cutoff. It is the inclusive cutoff that captures the true

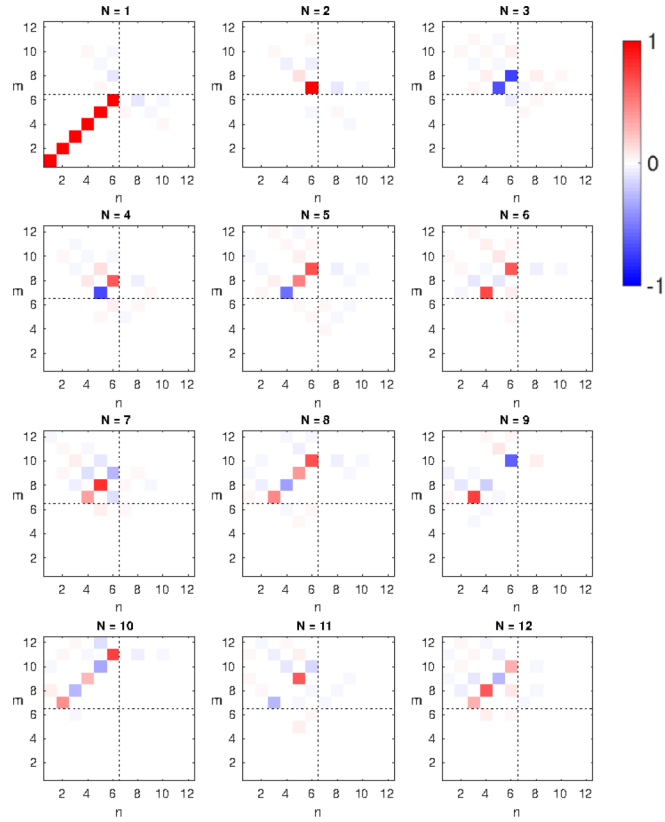

FIG. 5. Coulomb strength of $\lambda_{ee} = t$. The projection of the lowest 12 states onto each single-particle excitation of the ground state in the s.p. mode basis $\langle \Psi_N | a_m^\dagger a_n | \Psi_{GS} \rangle$ with removal mode n on horizontal axes and creation mode m on vertical axes. The off-diagonal lines are plasmonic behavior: Collective excitations in which many electrons all have the same momentum shift.

SPEC in these cases. Nonetheless, the behavior at other cutoff values give us insight into the meaning of the SPEC and why its sum over all states is discontinuous between the noninteracting and interacting cases.

Figures 3(a) and 3(b) show the rolling sum of the SPEC for small interactions with an exclusive (large $\epsilon_{G\text{-}S}$) cutoff and an inclusive (small $\epsilon_{G\text{-}S}$) cutoff, respectively. For a nonzero Coulomb interaction up to and including $\lambda_{ee} = t$ the behavior of the SPEC is remarkably similar for all interaction strengths, provided the inclusive cutoff is used. The SPEC is nearly a smooth function of eigenstate number (and of energy) with nearly all the nonzero SPEC occurring in the bottom quarter of the spectrum of eigenstates as shown in Fig. 2(c) for $\lambda_{ee} = t$. When a small enough cutoff is used, the rolling sums for $0 < \lambda_{ee}/t \leqslant 1$ fall on the same quasiuniversal curve which saturates at $m_e * (N_s - m_e)$. This shows that there are distinctly different behaviors between the noninteracting case and any case with interaction, no matter how small. For any value of a perturbing Coulomb interaction (no matter how small and up to $\lambda_{ee} = t$) the perturbation mixes excited states into the ground state, and single-particle excitation content is present in many more of the excited eigenstates. This discrete jump in the saturation value of the sum over SPEC points to the existence of small but well-defined excitations that come into existence in the presence of even the weakest interaction.

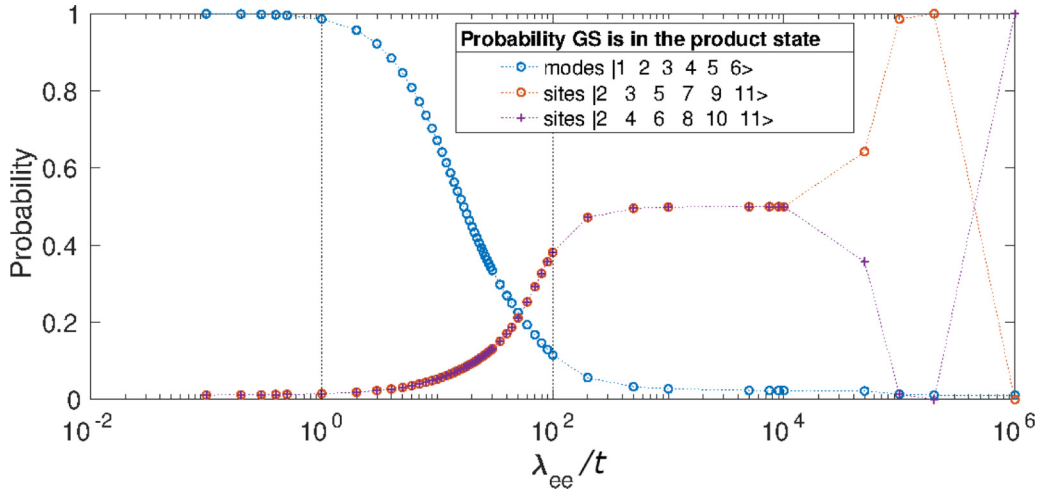

FIG. 6. Probability of measuring the interacting ground state in the ground states of the two limits $t = 0$ and $\lambda_{ee} = 0$.

This is consistent with the observation of Schulz [20] that the Wigner crystal (in continuous 1D systems) occurs for any Coulomb interaction strength and highlights the fundamental difference between weak interaction and no interactions.

As can be seen in Fig. 6 the ground state of the system in this regime still only has minute departures from the noninteracting limit: The overlap between the full ground state and the product state of the lowest six modes is nearly one. Yet those departures already have the defining character of the interacting ground state.

Previous authors identify this regime as a "metallic Wigner crystal" [21,23] or a "weakly pinned small-amplitude charge-density wave" [22]. Their focus is largely on whether the system is metallic in the thermodynamic limit, and by this measure their weakly interacting regime continues all the way to $\lambda_{ee}/t = 4$ or 5 where there is a crossover rather than a sharp transition. As we will see below, there is also something of a crossover in the behavior of the SPEC at that value. Characteristics ascribed to this phase include: metallic or quasimetallic (extrapolation to long chains gives a disappearing charge gap and high charge stiffness), a charge-density modulation that is small compared to the delocalized charge and disappears in the long chain limit and having strong departures from Luttinger liquid behavior that grow with λ_{ee}/t.

D. Very strong interaction $\lambda_{ee}/t \geqslant 100$

The region with the highest Coulomb interaction strengths is analogous to the small interaction case. However, now the occupation of particular sites in the chain is the applicable basis rather than the noninteracting single-particle modes being the relevant unperturbed basis. With an inclusive cutoff, the SPEC curves are all the same, up to the slight change in the order of a few of the levels. The SPEC curves for this region are shown in Figs. 3(c) and 3(d). The single-particle excitations are no longer confined to the low-energy part of the spectrum due to strong correlations induced by the extreme Coulomb interaction strength. Both the universal nature of the SPEC curve and the linear scaling of the energy levels with interaction strength seen in Fig. 1 point to the fact that the correlation is fully saturated: There is little reordering or mixing of levels as the interaction strength is varied. The Wigner crystal found at the extreme limit of no hopping is essentially present throughout this region.

We have defined the boundaries for the perturbative regions based on the dependence of the SPEC on the cutoff. However, Fig. 6 shows the probability of finding the ground state in the Wigner crystal of the $t = 0$ limit or the Slater determinant of the $\lambda_{ee} = 0$ limit as a function of the strength of the Coulomb interaction. The vertical lines indicating the perturbative regions from the SPEC analysis align with the regions of significant probability of finding the ground state in one of the limiting unperturbed ground states.

Previous authors refer to this regime as an "insulating charge-density wave" [21,23] or a "generalized Wigner lattice" [22]. It is characterized by a thermodynamically significant charge-density modulation and an insulating character (identified by a finite structure factor divided by chain length and a finite charge gap in long-chain extrapolation). As mentioned in the previous section, these authors identify this regime with $\lambda_{ee}/t > 4$ or 5. However, the charge-density modulation is fully saturated for $\lambda_{ee}/t \geqslant 100$. The next section will discuss the crossover regime between the regimes of weak and very strong interaction and the use of the charge-density-wave- (CDW-) and bond-order-wave- (BOW-) order parameters as measures for these regimes.

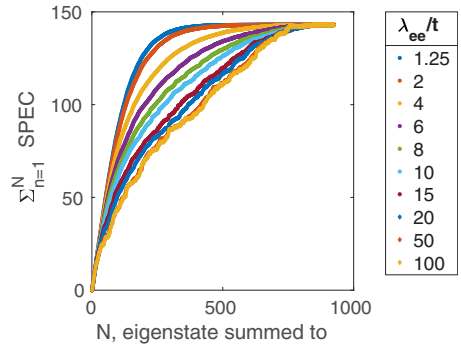

FIG. 7. Rolling sum of single-particle excitation content for eigenstates of a 12 atom chain with six electrons for nonperturbative region.

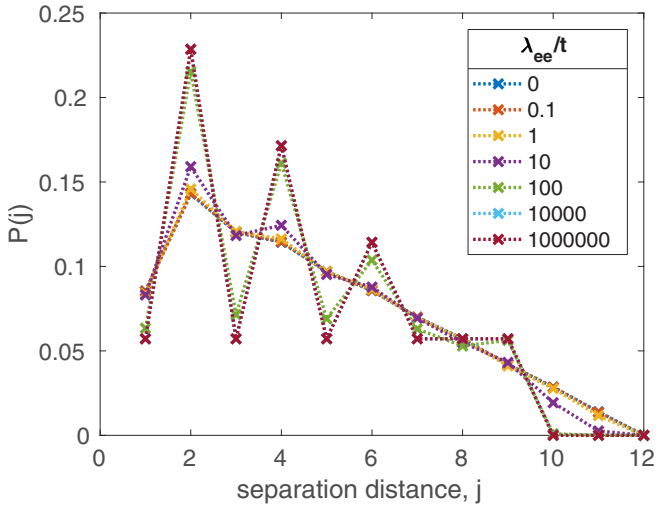

FIG. 8. Probability density of finding two electrons separated by a distance j for the ground state of six electrons on a 12 atom chain, varying the Coulomb interaction λ_{ee}, measured in units of the hopping t after Ref. [31].

E. Intermediate interaction: Onset and saturation of correlation $1 < \lambda_{ee}/t < 100$

In between the two perturbative regions is the region of increasing correlation. Correlation due to Coulomb repulsion causes the many-body eigenstates to cross and mix, and the ground state of the system is fundamentally changed. The single-particle excitation content is no longer sensitive to the cutoff used, giving the same results for a very wide range of values of $\epsilon_{G\text{-}S}$. The SPEC curves transition gradually between the quasiuniversal curves for the two perturbative regimes as seen in Fig. 7. However, as noted previously, the crossover assigned to $\lambda_{ee}/t = 5$ by Refs. [21–23] is visible in the SPEC curves as a transition from a mostly smooth curve in which single-particle excitations primarily make up low-energy eigenstates to a curve with discontinuities in which the single-particle excitations are not confined to the low-energy part of the spectrum.

That this is the region in which correlation sets in can be seen in Figs. 8 and 9. We use two measures of correlation: The first, used by Gambetta *et al.* [31] and Wang *et al.* [32], is the probability density of finding two electrons separated by a distance j,

$$P(j) = \sum_i \langle \Psi_{GS} | c_i^\dagger c_{i+j}^\dagger c_{i+j} c_i + c_i^\dagger c_{i-j}^\dagger c_{i-j} c_i | \Psi_{GS} \rangle. \quad (7)$$

We see in Fig. 8 that the departure from a linear decrease with distance grows in the intermediate region of Coulomb interaction ($\lambda_{ee}/t = 1 - 100$) and saturates at the upper limit of the region ($\lambda_{ee}/t = 100$) with evidence of every-other site occupation.

The second measure is the charge-density wave order parameter, defined by

$$O_{CD} = \sum_{\Delta i=1}^{N_s-1} \frac{(-1)^{\Delta i}}{(N_s - \Delta i)} \sum_{i=1}^{N_s-\Delta i} \langle \Psi_{GS} | c_i^\dagger c_i c_{i+\Delta i}^\dagger c_{i+\Delta i} | \Psi_{GS} \rangle. \quad (8)$$

As can be seen in Fig. 9, the charge-density wave order parameter maintains a constant value in the strong correlation regime but does not grow uniformly throughout the regime of onset and saturation of correlation.

This crossover region also sees the development and disappearance of bond-order oscillations. A bond-order wave is a state of broken symmetry in which the expectation value of the kinetic-energy operator alternates between every two-nearest-neighbor sites. Its order parameter is defined by

$$O_{BO} = \sum_{\Delta i=1}^{N_s-1} \frac{(-1)^{\Delta i}}{(N_s - \Delta i)} \sum_{i=1}^{N_s-\Delta i-1} \langle \Psi_{GS} | (c_i^\dagger c_{i+1} + c_{i+1}^\dagger c_i) \times (c_{i+\Delta i}^\dagger c_{i+\Delta i+1} + c_{i+\Delta i+1}^\dagger c_{i+\Delta i}) | \Psi_{GS} \rangle. \quad (9)$$

This order parameter measures the asymmetry of the bond strengths for odd and even bonds (odd bonds being those between the first and the second sites, the third and the fourth, etc.). A bond-order wave phase is defined as the existence of this order parameter in the infinite-chain length limit, which we do not evaluate here. (Finite Luttinger liquid systems exhibit bond-order oscillations that are not thermodynamically significant [33].) Discussions of the bond-order wave phase may be found in Refs. [33–35]. The Supplemental Material [26] and references therein [36–42] discuss our choice of order parameter.

One way to interpret the bond-order wave in a finite chain is as a charge-density wave which is shifted to lie between the sites. With this interpretation, Fig. 9 shows the growth of charge-density order with increasing interaction strength.

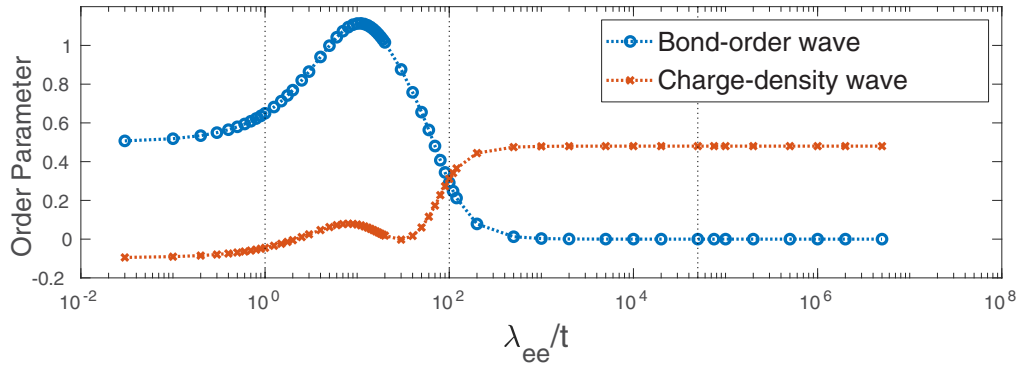

FIG. 9. BOW- and CDW-order parameters of the ground state as a function of Coulomb interaction strength.

Figure 7 shows that for smaller interaction strength (approximately $\lambda_{ee}/t \leqslant 4$) all low-energy excited states are primarily single-particle excitations, and higher-energy states are primarily multiple-particle correlated excitations. This reflects the low correlation seen in the order parameter (Fig. 9) and probability of separation (Fig. 8). The rolling sum of the SPEC is a smooth function of eigenstate number, implying that multiple-particle excitations are being mixed into all states smoothly as a result of interactions. As the interaction becomes stronger, lower-energy states gain multiple-particle excitation content, and higher-energy states gain single-particle excitation content as correlations develop. For the strongest interactions, neighboring excited states with nearly the same energy can have much different single-particle excitation content, and many more states in the low part of the spectrum have nearly zero SPEC (because moving two or more electrons simultaneously is both lower in energy once they are correlated and is very close to being an exact eigenstate of the system once Wigner crystallization has set in). Thus, the previously smooth curve of the rolling sum of the SPEC becomes rough as the SPEC of two consecutive eigenstates take very differing values.

III. CONCLUSION

We have considered small finite systems of interacting electrons with an eye toward what they can reveal about extended many-body physics. As quantum analog simulation in small systems develops experimentally, we expect that experiment coupled with such numerical analysis will enable a clearer understanding of large-scale phenomena and greater design capability. Understanding the nature of excited states is crucial for designing active systems, which will necessarily leave their ground state.

Using the single-particle excitation content of the excited states of a many-electron Hamiltonian we have identified five regimes in the parameter space of the Hamiltonian. This identification is largely consistent with and supplements previous analyses of the ground-state phase space of this system. This is, in part, because the possible single-particle excitations out of an interacting ground state reflect the nature of that ground state. We observe unique signatures in the SPEC of the eigenstate spectrum which allow us to identify the noninteracting and no-hopping regimes, perturbative regimes around each of those, and a broad crossover region between them in which correlation grows and saturates. As shown in the Supplemental Material [26], these signatures persist upon varying the range of interactions, the filling (number of electrons), the exchange fraction, and the size of the chain. This suggests that the behavior might be similar for other systems, for example, in higher-dimensional geometries or other forms of Hamiltonian.

When the rolling sum of the SPEC of the excited states has a universal curve as a function of eigenstate number and is sensitive to the cutoff for including minute quantities of a single-particle excitation in the vector space, the Hamiltonian is in a perturbative regime near a limit with a separable ground state (one that can be written as a Slater determinant of single-particle states). As strongly correlated behavior reorders and redefines the eigenstates the curve of the SPEC varies as well.

Small systems provide the opportunity for exact analysis of the entire spectra, finding all of the excitations of the systems. We have shown how this analysis provides new ways to define the different regimes of the many-body interactions and correlations, clearly identifying distinct differences that arise when interactions are turned on or hopping is turned off and the quasiuniversal behavior that arises in the perturbative regimes of weak interaction or weak hopping. Exact analysis of small systems and determination of the full spectrum of excitations also provides an opportunity to develop a full analysis of the dynamics of these systems.

[1] J. G. Bohnet, B. C. Sawyer, J. W. Britton, M. L. Wall, A. M. Rey, M. Foss-Feig, and J. J. Bollinger, Quantum spin dynamics and entanglement generation with hundreds of trapped ions, Science **352**, 1297 (2016).

[2] J. Zhang, G. Pagano, P. W. Hess, A. Kyprianidis, P. Becker, H. Kaplan, A. V. Gorshkov, Z.-X. Gong, and C. Monroe, Observation of a many-body dynamical phase transition with a 53-qubit quantum simulator, Nature (London) **551**, 601 (2017).

[3] H. Bernien, S. Schwartz, A. Keesling, H. Levine, A. Omran, H. Pichler, S. Choi, A. S. Zibrov, M. Endres, M. Greiner, V. Vuletić, and M. D. Lukin, Probing many-body dynamics on a 51-atom quantum simulator, Nature (London) **551**, 579 (2017).

[4] L. Tarruell and L. Sanchez-Palencia, Quantum simulation of the Hubbard model with ultracold fermions in optical lattices, C. R. Phys. **19**, 365 (2018).

[5] T. Hensgens, T. Fujita, L. Janssen, Xiao Li, C. J. Van Diepen, C. Reichl, W. Wegscheider, S. Das Sarma, and L. M. K. Vandersypen, Quantum simulation of a Fermi–Hubbard model using a semiconductor quantum dot array, Nature (London) **548**, 70 (2017).

[6] J. Salfi, J. A. Mol, R. Rahman, G. Klimeck, M. Y. Simmons, L. C. L. Hollenberg, and S. Rogge, Quantum simulation of the Hubbard model with dopant atoms in silicon, Nat. Commun. **7**, 11342 (2016).

[7] J. Wyrick, X. Wang, R. V. Kashid, P. Namboodiri, S. W. Schmucker, J. A. Hagmann, K. Liu, M. D. Stewart, C. A. Richter, G. W. Bryant, and R. M. Silver, Atom-by-atom fabrication of single and few dopant quantum devices, Adv. Funct. Mater. **29**, 1903475 (2019).

[8] N. H. Le, A. J. Fisher, and E. Ginossar, Extended Hubbard model for mesoscopic transport in donor arrays in silicon, Phys. Rev. B **96**, 245406 (2017).

[9] J. Preskill, Simulating quantum field theory with a quantum computer, in *Proceedings of The 36th Annual International Symposium on Lattice Field Theory — PoS(LATTICE2018)* (2019), Vol. 334, p. 024.

[10] S. McArdle, S. Endo, A. Aspuru-Guzik, S. C. Benjamin, and X. Yuan, Quantum computational chemistry, Rev. Mod. Phys. **92**, 015003 (2020).

[11] D. Wecker, M. B. Hastings, N. Wiebe, B. K. Clark, C. Nayak, and M. Troyer, Solving strongly correlated electron models on a quantum computer, Phys. Rev. A **92**, 062318 (2015).

[12] D. Loss and D. P. DiVincenzo, Quantum computation with quantum dots, Phys. Rev. A **57**, 120 (1998).

[13] E. Wigner, On the interaction of electrons in metals, Phys. Rev. **46**, 1002 (1934).

[14] Z. Eldredge, Z.-X. Gong, J. T. Young, A. H. Moosavian, M. Foss-Feig, and A. V. Gorshkov, Fast Quantum State Transfer and Entanglement Renormalization Using Long-Range Interactions, Phys. Rev. Lett. **119**, 170503 (2017).

[15] J. Eisert, M. Cramer, and M. B. Plenio, Colloquium: Area laws for the entanglement entropy, Rev. Mod. Phys. **82**, 277 (2010).

[16] L. F. Santos and M. Rigol, Onset of quantum chaos in one-dimensional bosonic and fermionic systems and its relation to thermalization, Phys. Rev. E **81**, 036206 (2010).

[17] J. M. Luttinger, An exactly soluble model of a many-fermion system, J. Math. Phys. **4**, 1154 (1963).

[18] T. Giamarchi, *Quantum Physics in One Dimension* (Clarendon, Oxford, 2003).

[19] K. Schönhammer, Physics in one dimension: Theoretical concepts for quantum many-body systems, J. Phys.: Condens. Matter **25**, 014001 (2013).

[20] H. J. Schulz, Wigner Crystal in One Dimension, Phys. Rev. Lett. **71**, 1864 (1993).

[21] S. Capponi, D. Poilblanc, and T. Giamarchi, Effects of long-range electronic interactions on a one-dimensional electron system, Phys. Rev. B **61**, 13410 (2000).

[22] B. Valenzuela, S. Fratini, and D. Baeriswyl, Charge and spin order in one-dimensional electron systems with long-range Coulomb interactions, Phys. Rev. B **68**, 045112 (2003).

[23] Z.-H. Li, Ground states of long-range interacting fermions in one spatial dimension, J. Phys.: Condens. Matter **31**, 255601 (2019).

[24] J. Ren, W.-L. You, and X. Wang, Entanglement and correlations in a one-dimensional quantum spin-$\frac{1}{2}$ chain with anisotropic power-law long-range interactions, Phys. Rev. B **101**, 094410 (2020).

[25] J. Hubbard, Generalized Wigner lattices in one dimension and some applications to tetracyanoquinodimethane (TCNQ) salts, Phys. Rev. B **17**, 494 (1978).

[26] See Supplemental Material at http://link.aps.org/supplemental/10.1103/PhysRevB.103.195429 for a discussion of quasiparticle weight, our choice of order parameters and the similar behavior of the SPEC for systems varying by size, filling, exchange fraction, and interaction range.

[27] P. Coleman, *Introduction to Many-Body Physics*, 1st ed. (Cambridge University Press, New York, 2015).

[28] A. J. Schofield, Non-Fermi liquids, Contemp. Phys. **40**, 95 (1999).

[29] F. D. M. Haldane, 'Luttinger liquid theory' of one-dimensional quantum fluids. I. Properties of the Luttinger model and their extension to the general 1D interacting spinless Fermi gas, J. Phys. C: Solid State Phys. **14**, 2585 (1981).

[30] G. Bryant and E. Townsend, The birth of atomic-scale quantum plasmons (unpublished).

[31] F. M. Gambetta, N. Traverso Ziani, F. Cavaliere, and M. Sassetti, Correlation functions for the detection of Wigner molecules in a one-channel Luttinger liquid quantum dot, Europhys. Lett. **107**, 47010 (2014).

[32] J.-J. Wang, W. Li, S. Chen, G. Xianlong, M. Rontani, and M. Polini, Absence of Wigner molecules in one-dimensional few-fermion systems with short-range interactions, Phys. Rev. B **86**, 075110 (2012).

[33] T. Mishra, J. Carrasquilla, and M. Rigol, Phase diagram of the half-filled one-dimensional $t - V - V'$ model, Phys. Rev. B **84**, 115135 (2011).

[34] G.-H. Liu and C.-H. Wang, Existence of bond-order-wave phase in one-dimensional extended hubbard model, Commun. Theor. Phys. **55**, 702 (2011).

[35] K. Hallberg, E. Gagliano, and C. Balseiro, Finite-size study of a spin-1/2 Heisenberg chain with competing interactions: Phase diagram and critical behavior, Phys. Rev. B **41**, 9474 (1990).

[36] M. Nakamura, Tricritical behavior in the extended Hubbard chains, Phys. Rev. B **61**, 16377 (2000).

[37] S. Ejima and S. Nishimoto, Phase Diagram of the One-Dimensional Half-Filled Extended Hubbard Model, Phys. Rev. Lett. **99**, 216403 (2007).

[38] H. Ding and Y. Wang, Bond-located phases driven by exchange interaction in the one-dimensional t-U-V-J model, Phys. Lett. A **375**, 1751 (2011).

[39] Y. Z. Zhang, Dimerization in a Half-Filled One-Dimensional Extended Hubbard Model, Phys. Rev. Lett. **92**, 246404 (2004).

[40] P. Sengupta, A. W. Sandvik, and D. K. Campbell, Bond-order-wave phase and quantum phase transitions in the one-dimensional extended Hubbard model, Phys. Rev. B **65**, 155113 (2002).

[41] C. Shao, H. Lu, H.-G. Luo, and R. Mondaini, Photoinduced enhancement of bond order in the one-dimensional extended Hubbard model, Phys. Rev. B **100**, 041114(R) (2019).

[42] M. C. Tran, J. R. Garrison, Z.-X. Gong, and A. V. Gorshkov, Lieb-Robinson bounds on n-partite connected correlation functions, Phys. Rev. A **96**, 052334 (2017).